Hirakawa, D., Nojiri, M., Aizawa, H., Tatsuoka, F., Sumiyoshi, T., and Uchimura, T. (2007). "Residual earth pressure on a retaining wall with sand backfill subjected to forced cyclic lateral displacements." *Measurement, Modeling & Analysis Geotech. Sym.*, 865-874.

Huntley, S.A., and Valsangkar, A.J. (2013). "Field monitoring of earth pressures on integral bridge abutments." *Canadian Geotechnical Journal*, 50:841-857.

Laman, J.A., and Kim, W.S. (2009). *Monitoring of integral abutment bridges and design criteria development.* Report No. PA-2009-005-PSU 002, Pennsylvania DOT, Harrisburg, PA.

Lehane, B.M. (2011). "Lateral soil stiffness adjacent to deep integral bridge abutments." *Geotechnique*, 61(7):593-603.

Morsy, A.M., Zornberg, J.G., Christopher, B.R., Leshchinsky, D., Tanyu, B.F., and Han, J. (2017), "Experimental approach to characterize soil-reinforcement composite interaction." *Proc. of 19th ICSMGE*, ISSMGE, Seoul, Korea.

Springman, S.M., Norrish, A.R.M., and Ng, C.W.W. (1996). *Cyclic loading of sand behind integral bridge abutments*. Report 146, Transport Research Laboratory (TRL), UK.

Sugimoto, T., Sumiyoshi, T., Sasaki, S., Hiroshima, M., and Yamamura, H. (2003), "Increase in the earth pressure by cyclic displacement of wall." *Proc. of Geotechnical Engineering in Urban Construction, Sino-Japanese Sym. on Geotech. Eng.*, 189-196.

Paik, K.H., and Salgado, R. (2003). "Estimation of active earth pressure against rigid retaining walls considering arching effects." *Geotechnique*, 53(7):643-653.

Comparison of Measurements and Limit State Solutions for Soil Pressures on Deep Flexible Underground Structures

Lohrasb Keykhosropour, S.M.ASCE[1],
and
Anne Lemnitzer, A.M.ASCE[2]

[1]Ph.D. Student, Department of Civil and Environmental Engineering, University of California, Irvine, CA, 92647; e-mail: lkeykhos@uci.edu
[2]Assistant Professor, Department of Civil and Environmental Engineering, University of California, Irvine, CA, 92647; e-mail: alemnitz@uci.edu

ABSTRACT

Understanding the magnitude and distribution of earthquake induced soil pressures is an important concern in designing retaining walls and underground structures. Seismic soil pressures on flexible and yielding structures are mainly analyzed through limit-state methods. To develop better understanding of these methods and their accuracy, a series of large-scale shake table tests was performed. A unique system of vertical underground structures was placed in an 8 m-diameter laminar soil box and embedded in a two-layered soil strata. The system was subjected to sinusoidal motions and scaled ground motion records of the Kobe 1995 earthquake. Apparent soil pressure records for different acceleration levels were analyzed and compared with classical and recently developed limit-state methods for both cohesionless and cohesive (c-φ) soil layers. Results indicate that all limit-state methods under-predicted seismic pressures at small to moderate accelerations (<0.4g). This paper will provide a brief review of limit state methods in literature followed by an overview of the experimental program, the data analysis, and a discussion of the suitability of existing methods in predicting pressures on flexible underground structures.

INTRODUCTION

Earthquake induced soil pressures on earth retention systems and underground elements, such as embedded structures, pipelines, and infrastructure components are critical analysis components for the nonlinear evaluation of dynamic soil-structure interaction. The correct assessment of magnitude and distribution has been a controversial research area for decades, and sparked the development of numerous methodologies using simplified or extensive numerical procedures.
Current retaining structures are divided into "yielding" and "non-yielding" systems based on their relative movement to the soil. According to FEMA 750 (2009), the movement of the retaining structure's tip determines its classification into either "non-yielding" or "yielding" structures, the latter one applying when wall displacements exceed 0.002 times the structure's height (Fig. 1). Accordingly the condition for the development of minimum active pressures is provided and the wall is called "yielding"; in turn, "non-yielding" walls do not satisfy this criterion (e.g., basement walls). Limit-state methods typically known through the well-known

Mononobe-Okabe (M-O) method (Mononobe and Matsuo 1929; Okabe 1926) and its modified version, i.e., the Seed-Whitman (S-W) method (Seed and Whitman 1973) are primarily used for evaluating seismic soil pressures on yielding walls.

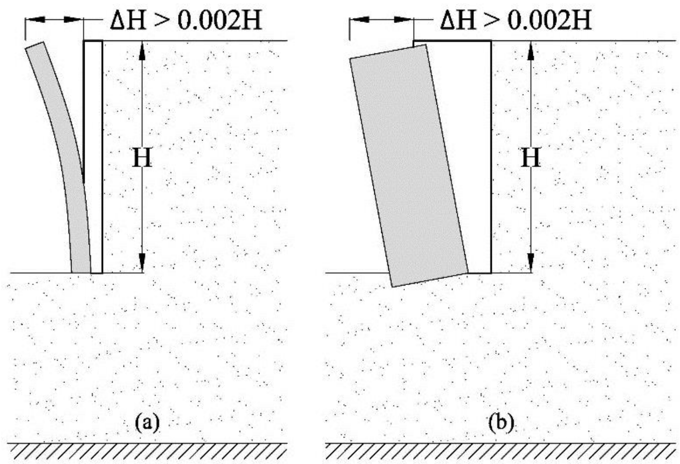

Fig. 1. Yielding Retaining Walls: (a) flexible; (b) rigid

Upon briefly reviewing the historic development of limit state approaches, this paper will investigate the applicability of these methods on flexible underground structures that differ from typical "yielding walls" documented in literature. Vertical underground structures are different in geometry and overall structural bending behavior and are often less frequently present in current construction compared to traditional retaining walls. Nevertheless, vertical underground structures gain increased popularity in dense, urban settings to facilitate multi-level infrastructure connectors (i.e. elevator structures) or expand industrial and commercial space to sub-surface locations. Large-scale shake table tests performed on underground structures at the E-Defense facility in Miki, Japan, will serve as the experimental reference for this paper. The objective of this manuscript is to investigate the suitability of different traditional and recently developed limit-state methods for both cohesionless and cohesive (c-φ) soils in predicting the seismically induced earth pressures experimentally measured on the deep flexible underground structures.

Review of Limit-State Methods for Cohesionless Soils

The limit-state approach uses a pseudo-static analysis and considers the soil to be perfectly plastic. Solutions of the problem are categorized into two groups: stress solutions and kinematic solutions (Mylonakis et al. 2007). The stress solutions, which are based on classical Rankine equations, utilize the stress states to satisfy the field equations of equilibrium and boundary conditions and also comply with the predefined failure criterion. The stress solution for cohesionless soils in seismic conditions is only used by Mylonakis et al. (2007).
Coulomb's theory (1776) for calculating static lateral earth pressures is the basis of the kinematic solution. Mononobe and Matsuo (1929) and Okabe (1926), where the first researchers who translated Coulomb's original formulations into an approach suitable for determining dynamic lateral earth pressures on retaining structures. In this approach, the earthquake loading is applied to the soil through pseudostatic horizontal (k_hg) and vertical (k_vg) accelerations. The total

seismic active thrusts, P_{ae}, which includes both static and seismic increment forces is calculated based on the Coulomb wedge theory and is equal to:

$$P_{AE} = 0.5\gamma H^2(1 - k_v)K_{AE} \quad (1)$$

where

$$K_{AE} = \frac{\cos^2(\varphi - \theta - \beta)}{\cos\theta\cos^2\beta\cos(\delta + \beta + \theta)\left[1 + \sqrt{\frac{\sin(\varphi + \delta)\sin(\varphi - \theta - i)}{\cos(\delta + \beta + \theta)\cos(i - \beta)}}\right]^2} \quad (2)$$

In the above equation, γ is the unit weight of the soil, H is the height of the wall, φ is the soil friction angle, δ is the angle of wall friction, i is the slope of ground surface behind the wall, β is slope of the back of the wall to vertical, and $\theta = \tan^{-1}\left(\frac{k_h}{1 - k_v}\right)$.

The M-O method does not provide the seismic stress distribution profile and similar to Coulomb, is only intended to estimate the total seismic force acting on the wall. Mononobe and Okabe suggested that the location of the P_{AE} is at the same position as the static active force at H/3 from the base of the wall. A limiting problem with the M-O method is Eq. 2, which does not converge in cases where $\theta < \varphi - \beta$. For common soil friction angles this issue becomes problematic when accelerations exceed 0.7g (Sitar et al., 2012).

After analyzing a variety of shake table experiments and conducting accompanying parametric studies, Seed and Whitman (1970) concluded that the increase of lateral pressure due to the base excitation is higher near the top of the wall and the resultant seismic increment acts between 0.5H to 0.67H above from the base. Based on this conclusion and in order to solve the convergence problem of (Eq. 2), Seed and Whitman updated the M-O method by separating the total force into static, P_A, and dynamic, $\Delta P_{AE} = 1/2\gamma H^2 \Delta K_{AE}$, components. They also introduced the term "inverted triangle' for the distribution of dynamic pressures increment by recommending that the resultant of the dynamic increment is applied at the 0.6H from the base.

Based on the results of a series of centrifuge tests, Steedman and Zeng (1991) developed a simple pseudo-dynamic method which considers the shear wave velocity of the backfill and frequency of the applied motion. The magnitude of the total earth pressure is similar to M-O, but the point of application of the dynamic thrust is higher than H/3 above the base, and depends on the motion's frequency, and soil properties (Steedman and Zeng, 1991). In 2007, Mylonakis et al. developed a closed-form stress solution for gravitational and seismic induced earth pressures on retaining walls with cohesionless backfills for both active and passive conditions. Mylonakis et al. divided the backfill into two regions with different stress fields; one region close to the soil surface and the second one close to the wall. In both conditions, the soil is assumed to resist against yielding (Mohr-Coulomb criterion) under combined action of gravity and seismic forces. Resultant lateral forces in static and dynamic cases are treated separately and the dynamic force increment is determined as their difference. This approach is mathematically correct but its physical meaning is limited because the stress fields and their corresponding failure surfaces are different in gravitational and seismic problems. The lateral earth pressure distribution is assumed to be linear, and in absence of the surcharge the point of application of the resultant force is at H/3 above the base.

Limit-State Methods for Cohesive Soils

About 40 years after the M-O method was published, Prakash and Saran (1966) and Saran and Prakash (1968) developed a general solution for seismic pressures on retaining walls supporting c-φ soils. In their method, the vertical component of the earthquake acceleration was ignored. Consecutive studies by Richards and Shi (1994) proposed a solution to predict seismic stresses in the free field due to inertial forces. This solution included both, horizontal and vertical accelerations, and is applicable to homogenous backfills of Coulomb-type material. Normal and shear surface tractions are also included in this method of analysis. Shukla et al. (2009) developed the M-O concept for c-φ soils to obtain a single critical failure wedge surface, disregarding the friction/adhesion between the wall and the retaining backfill. This method was later modified by Shukla and Bathurst (2012) to consider the effect of adhesion between the wall and soil, as well as tension cracks in the backfill material. Since this method uses the kinematic solution approach, the distribution of lateral soil pressures cannot be obtained directly and earth pressures are assumed to vary linearly behind the wall. The point of application of the resultant force is therefore located at H/3 from the base of the wall. In 2013, Iskander et al. extended the classic Rankine solution to predict seismic active earth pressures behind inclined rigid walls supporting sloped c-φ backfills. The effect of the inertial forces is accounted for by altering the static gravity acceleration. This method accounts for the wall inclination and backfill slope, and contrary to kinematic solutions (e.g., Saran and Prakash 1966, Shukla 2012), is capable of providing the distribution of lateral seismic stresses behind the wall as well as the tension crack length. However, this method ignores the soil-wall adhesion and assumes that the stress state adjacent to the wall is the same as the free field. The soil-wall friction angle is simply computed based on the equilibrium of soil elements near the wall, which according to Iskander et al. (2013) yields erroneous results, but is ignored by the authors for simplicity.

Shamsabadi et al. 2013 proposed a Log-Spiral-Rankine (LSR) model with a composite failure surface including a logarithmic spiral curve and a linear section (Rankine) to evaluate active and passive seismic soil pressures in $c - \varphi$ soils. The geometry of the curvilinear failure surface was obtained based on three different stress states in two different zones: the logarithmic spiral region and the Rankine zone. In 2015, Xu et al. improved the aforementioned model. This method is suitable for analyzing problems with maximum horizontal acceleration of $k_h = 0.3535$ g.

The following methods were used to compare analytical predictions with experimental data: M-O method, S-W method, Mylonakis et al., Richards and Shi, and finally, Iskander et al. The Xu et al method cannot be used to predict the experimental data, as the applied ground motions in the experiment exceed the range of input motions under which the Xu et al model performs reliably.

Experimental Setup and Material Properties

The experimental studies were executed at the E-Defense facility in Miki, Japan. A system of fully instrumented underground structures (Fig. 2) was installed in a circular laminar box and embedded into a two-layered soil stratum with a total thickness of 6m. The soil-structure system was subject to sine sweep motions and scaled ground motion records of the Kobe (1995) earthquake. The model structures were built from aluminum (E = 70.1 GPa, $\nu = 0.36$) at 1/20 of their corresponding prototypes' sizes and bending stiffness. The vertical shafts with dimensions of 0.8m square and 12mm in thickness had a total height of 7m and were spaced 4.80 m apart (center to center) and connected through a horizontal cut-and-cover tunnel with dimensions of 0.6 m in width and 0.3 m in height. The connections between the tunnel and the vertical shafts were constructed as rigid and flexible joints. A detailed description of the test setup and structural elements can be found in Lemnitzer et al. 2017. Of interest to this study is the vertical shaft located on the left of the model layout in Figure 2 (see highlights shaft side). This shaft was instrumented with 20 load-cell based pressure cells with two different capacities (i.e., 144 kPa and 288 kPa). Details on this instrumentation can be found in Keykhosropour et al. (2017).

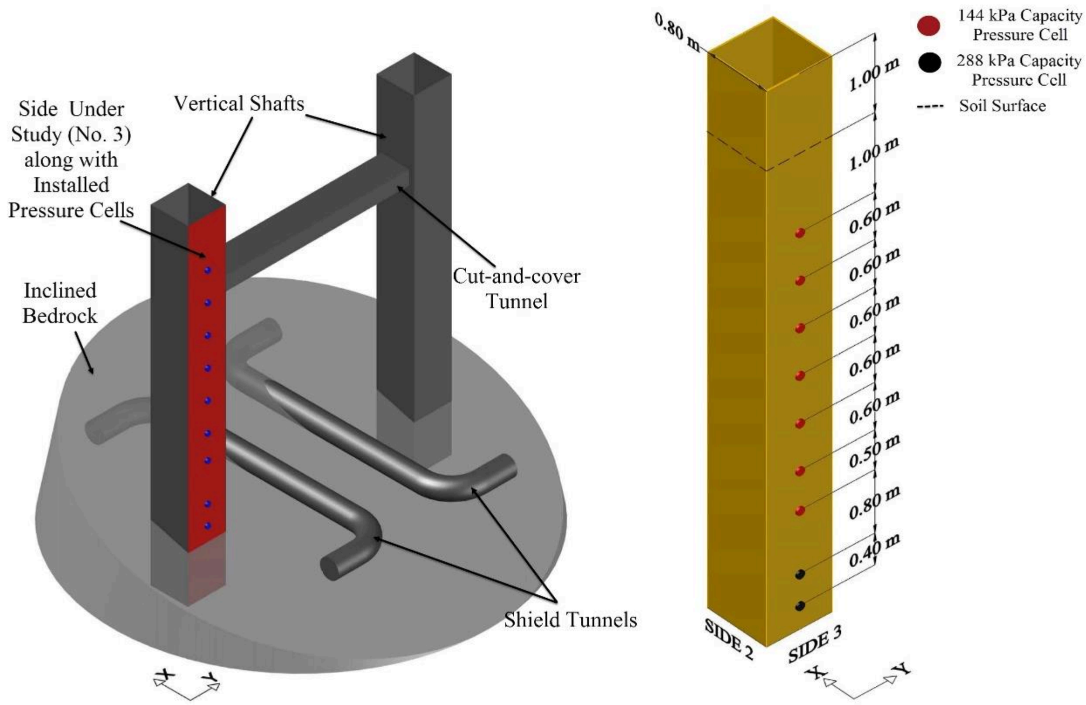

Fig. 2. Test setup and instrumentation of the shaft side used for this study (No. 3)

The laminar box was filled with a two-layer soil system: the upper layer was 4.90 m thick and consisted of Albany silica sand ($D_r = 54.05\%$; $\gamma = 16.59\ kN/m^3$) overlying a stiffer inclined layer consisting of cemented sandy soil with a maximum height of 2.2 m. The cemented soil layer was intended to replicate bedrock. Properties of the soil materials were obtained through laboratory and on-site testing at E-Defense (e.g., CPT and shear wave velocity measurements). Cohesion and friction angle of the top layer (sand layer) were measured though consolidated undrained (CU) triaxial testing for different relative densities and at different confining pressures. A cohesion of 17 kPa and friction angle of 35.51° were obtained.Unconfined compression testing on samples of the cemented soil layer revealed compressive strengths of 1298 kPa. Cohesion and frictional angle of this layer were not measured directly, but assumed to be equal to the frictional angle of the first layer, i.e., 35.51°.This assumption is suggested by Maalej et al., 2007, who studied sand-cement mixtures experimentally and found that mixing the sand with cement does not influence the frictional angle significantly and proposed the amount of cohesion to be proportional to the volume fraction of the cement in the mixture. Therefore, the cohesion of it was calculated equal to 334 kPa. The average unit weight for this layer was estimated to be 20.59 kN/m^3.

Applied Motions & Corresponding Pressures

The container model was excited using different ground motions applied to the shake table: (1) 50% and 80% scaled ground motions from the 1995 Kobe earthquake recorded at the JR Takatori Station (N34.651339, E135.135203), and (2) stepped sine sweeps in different horizontal directions (e.g., X, Y). Step sine motions were applied to characterize the dynamic response of the model at various acceleration levels, while the ground motions allowed for the nonlinear performance assessment of the model under dynamic loading. Sample data obtained during the 50% Kobe motion are depicted in Figure 3a-e. Figure 3a shows the acceleration at the base of the container in X direction, Figure 3b – 3e show the pressure time-histories on side 3 of the shaft. Please note that these pressures only represent the seismic increment, and do not include static pressures at rest (i.e., before shaking). All initial pressures were “zeroed”, hence, pressure time histories vary in signage (+/-). Figure 3 indicates an increase in pressure amplitudes with increasing depth, and a consistently increasing accumulation of residual pressures against the vertical shaft. These residual pressures are important as they remain at approximately 75% of the transient dynamic pressures observed during the ground motion. The residual stresses can be attributed to the densification of the soil layer during shaking and an increase of relative density from D_r = 54.05% to D_r = 71.95% prior and after testing, respectively. This effect was also manifested in surface settlements of 6.70 cm settlement at the ground surface.

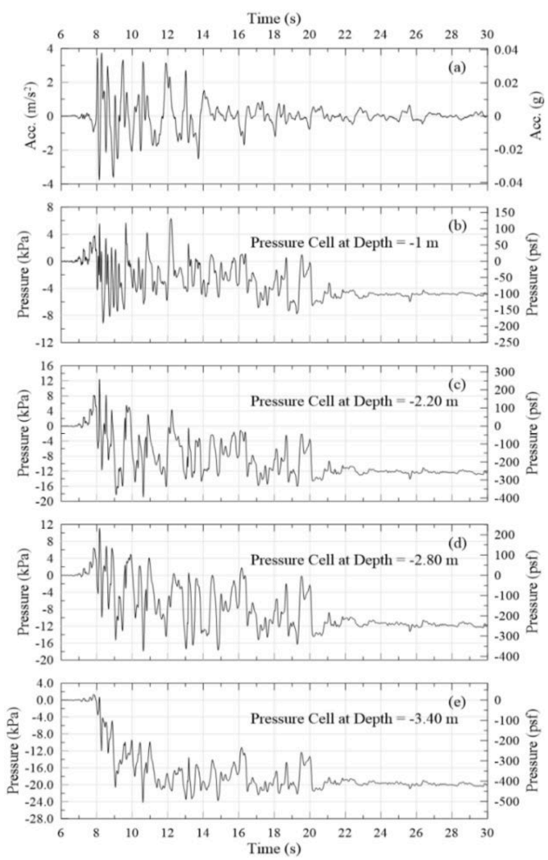

Fig. 3. Acceleration and pressure time histories recorded during the 50% Kobe motion

Comparison of Experimental Results with Analytical Formulations

The seismic soil pressure profiles on side 3 of the rigid vertical shaft for the 50% Kobe motion were obtained by combining the maximum pressure recordings during the ground motion at each respective location. As mentioned before, the Mononobe-Okabe (M-O), Seed and Whitman (S-W) and Mylonakis et al. (2007) methods were selected as representative choice for cohesionless pressure models; Richards and Shi (1994) and Iskander et al. (2013) were used as methods that consider cohesion.

In the methods which only consider the friction angle of the soil material, the soil material was modeled as a uniform layer with the equivalent unit weight, (c=0, φ=35.51°, γ=17.33 kN/m^3). In the methods that consider cohesion, the properties of both layers were included in the analyses. It should be noted that all of these methods were originally developed for uniform, single layered $c - \varphi$ backfills. In order to make Iskander et al. (2013) and Richards and Shi (1994) applicable to our experiment, the analytical approaches suggested by the authors were applied to both soil layers, and overburden stresses were calculated accordingly, i.e., the respective layer properties were utilized to determine the overburden stress in the cemented layer. The stress state of each depth should comply with the Mohr-Coulomb failure criterion using the mechanical properties (i.e., cohesion and friction angle) of that depth.

The distribution of the experimentally obtained seismic lateral earth pressures is shown in Figure 4. A 3rd degree polynomial fit is provided through the data. Pressures increase with increasing depth and experience an abrupt jump at the soil-rock interface. This trend is typical for structures with bottom fixity. The total pressure resultant was back-calculated as the area of distributed pressures along the wall and resulted in 109.40 kN. The point of application of the resultant force, h, was obtained using the area underneath the fitting curve and was determined to be 2.50 m from the base of the wall (h/H = 0.416).

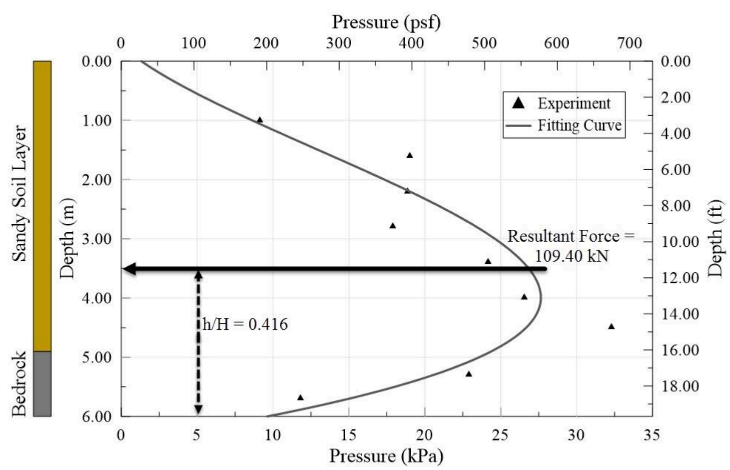

Fig. 4. Distribution of recorded earth pressures for the 50% motion

A comparison with the limit-state methods for the 50% ground motion is presented in Figure 5. In addition, Table 1 provides a summary of the resultant forces, their point of application and corresponding moments calculated for all limit-state methods.

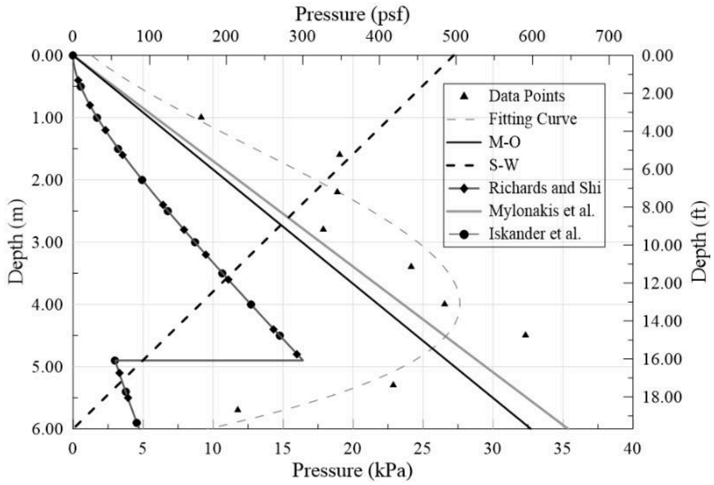

Fig. 5. Comparison of the distribution of seismic lateral earth pressures obtained from limit-state methods with the experimental results for the 50% motion

Table 1. Summary of the results of elastic-based methods and their comparison with experimental data for 50% and 80% motions

	Ground Motion		
	Kobe EQ - 50% Motion		
	Resultant Force (kN)	Point of Application (h/H)	Resultant Moment[a] (kNm)
Experiment	109.4	0.416	273.06
M-O	98.12	0.333	196.04
S-W (1973)	81.58	0.6	293.69
Richards & Shi (1994)	38.71	0.387	89.88
Mylonakis et al. (2007)	106.1	0.333	211.99
Iskander et al. (2013)	38.72	0.387	89.91

[a] Resultant moment was calculated as the product of the resultant force and (h) with respect to the base

As it can be seen from Figure 5 and Table 1, all of the methods under-predicted the seismic pressures and the resultant force in the 50% motion. In terms of pressure distribution in the upper soil layer, the Mylonakis et al. solution provides closest approximation to the experimental data. None of the utilized methods could compute the correct location of the resultant force in the experiments. This is due to the fact that all of the limit-state methods consider the earthquake loading through the pseudo-static inertial forces and ignore the frequency characteristics of the applied motion which has a significant influence on the distribution and magnitude of seismic soil pressures.

It is also evident from Figure 3 that none of the Coulomb-based methods (i.e., with kinematic solution) could capture the soil layer change and predicted a simple linear distribution of seismic stresses. The only two methods which were capable of capturing the layer change were Richards and Shi (1994) and Iskander et al. (2013) which are Rankine-based and utilize the stress solution. It is interesting that these two methods provide the same values of seismic stresses along the wall although they use two different sets of assumptions and formulations. Unfortunately the results do not capture the pressure distribution well.

Based on Table 1 it can be seen that Mylonakis et al. 2007 produce the most similar resultant pressure (3% difference), followed by M-O (10% difference). Given the different assumptions for the location of the pressure resultant between the methods, the moments applied to the system differ broadly. Seed and Whitman over-predict the moment by 8%, while Mylonakis et al. 2007 under-predict the moment by 22%.

Please note that the peak ground acceleration for this scaled ground motion was 0.38g. Hence, the experimental results are somewhat contradicting the recommendations by previous researchers (e.g., Seed and Whitman 1970; Clough and Fragaszy 1977; Sitar et al. 2012) who believed that currently used methods are very conservative and lead to excessively conservative designs in regions where design PGA is below 0.4g. The measured distributed pressure profiles indicate a slightly higher pressure magnitude than those determined analytically. However, this issue can be attributed to the high flexibility of the structure in our experiments and the fact that all of the limit-state methods were developed for yielding rigid retaining structures.
For ground motions with higher accelerations, e.g. > 0.5g (not presented in this paper) a general trend of analytical over-prediction as indicated by the above references was confirmed.

Summary & Conclusion

Experimentally measured seismic soil pressures on flexible vertical underground structures were compared with limit state methods published in literature. Results confirmed that the flexibility of the structural component as well as the 3D soil-structure interaction effects are important contributors to the system performance and the development of seismic earth pressures. The general solutions for rigid retaining structures can only serve as rough estimate. Limit state methodologies in literature capture a pressure distribution and magnitude within a 25% range of accuracy. Furthermore, lack of limit state methods for multi-layer soil profiles pose a significant limitation to current analytical capabilities. More rigorous numerical tools (e.g. finite element and finite difference methods) are recommended for this unique type of structure if a reliable range of accuracy is desired.

References

Building Seismic Safety Council. (2010). NEHRP Recommended Provisions for Seismic Regulations for New Buildings and Other Structures (FEMA 750), 2009 Edition, Part 1 – Provisions. BSSC, Washington, DC.

Clough, G. W. and Fragaszy, R. F. (1977). “A Study of Earth Loadings on Floodway Retaining Structures in the 1971 San Fernando Valley Earthquake.” Proc. of the 6th World Conf. on Earthquake Eng., 3, 2455-2460.

Ghosh, S. and Saran, S. (2007). “Pseudo-static Analysis of Rigid Retaining Wall for Dynamic Active Earth Pressure.”, International Conf. on Civil Eng. In the New Millennium: Opportunity and Challenges (CENeM-2007) Bengal Eng. And Science University, Shibpur, West Bengal.

Ghosh, S., Dey, G. N., and Datta, B. (2008). “Pseudo-static Analysis of Rigid Retaining Wall for Dynamic Active Earth Pressure.” 12th International Conf. of International Association for Computer Methods and Advances in Geomechanics, Goa, India, 2008, 4122 – 4131.

Iskander, M., Zhibo, C., Omidvar, M., Guzman, I., and Elsherif, O. (2013). “Active Static and Seismic Earth Pressure for c-φ Soils.” Soils and Foundations, 53(5), 639-652